Chemical Science

ROYAL SOCIETY OF CHEMISTRY

EDGE ARTICLE

View Article Online
View Journal | View Issue

Cite this: *Chem. Sci.*, 2020, **11**, 6745

All publication charges for this article have been paid for by the Royal Society of Chemistry

Received 25th March 2020
Accepted 23rd May 2020

DOI: 10.1039/d0sc01740j

rsc.li/chemical-science

Transformations of the *cyclo*-P_4 ligand in $[Cp'''Co(\eta^4\text{-}P_4)]$†

Martin Piesch, Michael Seidl and Manfred Scheer *

The reactivity of the *cyclo*-P_4 ligand complex $[Cp'''Co(\eta^4\text{-}P_4)]$ (**1**) (Cp''' = 1,2,4-tri-*tert*-butylcyclopentadienyl) towards reduction and main group nucleophiles was investigated. By using $K[CpFe(CO)_2]$, a selective reduction to the dianionic complex $[(Cp'''Co)_2(\mu,\eta^3{:}\eta^3\text{-}P_8)]^{2-}$ (**2**) was achieved. The reaction of **1** with ^{t}BuLi and $LiCH_2SiMe_3$ as carbon-based nucleophiles yielded $[Cp'''Co(\eta^3\text{-}P_4R)]^-$ (R = ^{t}Bu (**4**), CH_2SiMe_3 (**7**)), which, depending on the reaction conditions, undergo subsequent reactions with another equivalent of **1** to form $[(Cp'''Co)_2(\mu,\eta^3{:}\eta^3\text{-}P_8R)]^-$ (R = ^{t}Bu (**5**), CH_2SiMe_3 (**8**)). In the case of **4**, a different pathway was observed, namely a dimerisation followed by a fragmentation into $[Cp'''Co(\eta^3\text{-}P_5{}^tBu_2)]^-$ (**6**) and $[Cp'''Co(\eta^3\text{-}P_3)]^-$ (**3**). With OH^- as an oxygen-based nucleophile, the synthesis of $[Cp'''Co(\eta^3\text{-}P_4(O)H)]^-$ (**9**) was achieved. All compounds were characterized by X-ray crystal structure analysis, NMR spectroscopy and mass spectrometry. Their electronic structures and reaction behavior were elucidated by DFT calculations.

Introduction

The parent organic carbon aromates C_nH_n have been widely used as ligands in organometallic chemistry in sandwich, half-sandwich or multi-decker sandwich complexes. While the majority of compounds include Cp (C_5H_5) and benzene (C_6H_6) as ligands, examples for complexes with C_3H_3 and C_4H_4 ligands are rather limited.[1] Due to the isolobal analogy of the CH unit and P, a large variety of ligands have been described where CH units were replaced partially by P atoms as in *e.g.* phospholes (C_4H_4P, $C_2H_2P_3$)[2] or phosphinines (C_5H_5P)[3] or completely resulting in aromatic *cyclo*-P_n ligands. While complexes with *cyclo*-P_3 (*e.g.* $[Cp^*Ni(\eta^3\text{-}P_3)]$,[4] $[(Cp'''Ni)_2(\mu,\eta^3{:}\eta^3\text{-}P_3)]$[5]), *cyclo*-$P_5$ (*e.g.* $[Cp^*M(\eta^5\text{-}P_5)]$ (M = Fe,[6] Ru[7]) $[(Cp^RM)_2(\mu,\eta^5{:}\eta^5\text{-}P_5)]$ (M = Cr,[8] Mn[9])) and *cyclo*-P_6 $[(Cp^RM)_2(\mu,\eta^6{:}\eta^6\text{-}P_6)]$ (M = Ti,[10] V,[11] Nb,[12] Mo,[13] W[11]) ligands have been known for decades, the *cyclo*-P_4 Co complex in this row was unknown for a long time. Recently, we succeeded in the synthesis of $[Cp'''Co(\eta^4\text{-}P_4)]$ (**1**).[14] This inspired the synthesis of other complexes containing *cyclo*-P_4 ligands a few of which were recently reported as *e.g.* being based on rare earth metals like $[\{(DippForm)_2Sm\}_2(\mu,\eta^4{:}\eta^4\text{-}P_4)]$,[15] group five metals, $[Cp^RM(CO)_2(\eta^4\text{-}P_4)]$ (M = V, Nb, Ta (**A**)),[16] on chromium, $[L_2Cr_2(\eta^2{:}\eta^2{:}\eta^1{:}\eta^1\text{-}P_4)]$ (L = (2,6-diisopropylphenyl)-{6-(2,6-dimethylphenyl)-pyridin-2-yl}-amide)),[17] on iron, $[^{Ph}PP_2{}^{Cy}Fe(\eta^4\text{-}P_4)]$ (**B**),[18] on molybdenum, $[(Ar^{Dipp}CN)_2Mo(CO)_2(\eta^4\text{-}P_4)]$ (**C**)[19] and on the anionic iron complex $[Cp^{Ar}Fe(\eta^4\text{-}P_4)]^-$ (ref. 20) as well as on the anionic cobalt complex $[(PHDI)Co(\eta^4\text{-}P_4)]^-$ (**D**).[21] The reactivity of these complexes was only little investigated by the coordination chemistry of **A** and **B** towards coinage metal salts[18,22] and the reactivity of **B** towards Lewis acids as for instance $B(C_6F_5)_3$ (Scheme 1).[18] The anionic compound **D** was quenched with phosphorus-based electrophiles (R_2PCl) leading to neutral complexes with substituted *cyclo*-P_5R_2 ligands (Scheme 1).[21] Ring expansion reactions were also reported for **1** using the pnictogenidene complexes $[Cp^*E\{W(CO)_5\}_2]$ (E = P, As), leading to neutral cobalt complexes with organo-

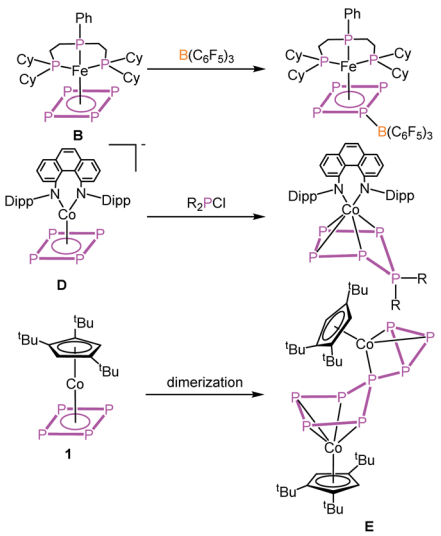

Scheme 1 Reactivity of selected *cyclo*-P_4 ligand complexes.

Institut für Anorganische Chemie, Universität Regensburg, 93040 Regensburg, Germany. E-mail: Manfred.Scheer@ur.de; Web: https://www.uni-regensburg.de/chemie-pharmazie/anorganische-chemie-scheer/

† Electronic supplementary information (ESI) available. CCDC 1984450–1984455. For ESI and crystallographic data in CIF or other electronic format see DOI: 10.1039/d0sc01740j

substituted *cyclo*-P_5 and *cyclo*-P_4As ligands,[23a] with the latter showing that reactions with electrophiles were investigated (other examples *cf.* ref. 23*b* and *c*), though not yet the reactivity towards nucleophiles or reduction reactions in general. As for the former chemistry, however, it was studied for $[Cp^*Fe(\eta^5\text{-}P_5)]$ and $[Cp^*Ni(\eta^3\text{-}P_3)]$,[5,24] for which organo-substituted anionic complexes of the types $[Cp^*Fe(\eta^4\text{-}P_5R)]^-$ and $[Cp'''Ni(\eta^2\text{-}P_3R)]^-$ were obtained.

With this state of the art in mind, questions arose as to how **1** would respond to redox reactions or to a nucleophilic attack. Would a dimerisation by a P–P bond formation or a simple substitution occur, as known from the reactions of other *cyclo*-P_n ligand complexes? Would a structural rearrangement be possible, including a reorganisation process? Moreover, controlling the reactivity of **1** is a challenging task since it has a high intrinsic tendency to dimerising irreversibly in solution to give a connected five- and three-membered P_8 ligand in $[(Cp'''Co)_2(\mu,\eta^4\text{:}\eta^3\text{-}P_8)]$ (**E**, Scheme 1).[14] Furthermore, there are only few examples known of four-membered heterocycles to undergo ring expansion reactions, *e.g.* by nucleophiles being added to phosphetanes[25] or by oxidizing the diphosphete complex $[Cp'''Co(\eta^4\text{-}P_2(C^tBu)_2)]$ to give the five- and three-membered ring products, $[Cp'''Co(\eta^5\text{-}P_3(C^tBu)_2)]^+$ and $[Cp'''Co(\eta^3\text{-}P(C^tBu)_2)]^+$, respectively.[26]

Herein we report the unprecedented transformations of the *cyclo*-P_4 ligand complex **1** upon reduction and the reactions with main-group nucleophiles to give novel P-rich ligand complexes.

Results and discussion

To obtain a first insight into the reactivity of **1**, the frontier molecular orbitals (*cf.* Fig. S32†) were computed by DFT calculations. They reveal that both HOMO and LUMO are mainly located on the *cyclo*-P_4 ligand and, hence, **1** should react with both electrophiles and nucleophiles. The reactivity of **1** towards electrophiles has been shown by reactions with $[Cp^*E\{W(CO)_5\}_2]$ (E = P, As).[23] On the other hand, the cyclic voltammogram (*cf.* Fig. S18†) of **1** in dme reveals a weak irreversible oxidation process at +275 mV and a strong irreversible reduction process at −2081 mV against $[Cp_2Fe]/[Cp_2Fe]^+$, indicating the potential ligand-centred redox activity of **1** (for details *cf.* ESI†).

Due to the low reduction potential of **1**, we used potassium, potassium graphite and potassium hydride for the chemical reduction. In all cases, the formation of a mixture of $[(Cp'''Co)_2(\mu,\eta^3\text{:}\eta^3\text{-}P_8)]^{2-}$ (**2**) and $[Cp'''Co(\eta^3\text{-}P_3)]^-$ (**3**)[27] in an approximate ratio of 1 : 1 (Scheme 2) is observed (*cf.* Fig. S1†). When the reaction is conducted in the presence of 18-c-6 or 2,2,2-cryptand, only **3** can be detected in the $^{31}P\{^1H\}$ NMR spectrum. The selective synthesis of **2** can be achieved by using $K[CpFe(CO)_2]$ at low temperatures. Interestingly, $K[CpFe(CO)_2]$ should not be able to reduce **1** (its reduction potential of −1800 mV in thf against $[Cp_2Fe]/[Cp_2Fe]^+$ is higher than that of **1** (*vide supra*)).[28] After workup, $[K(dme)]_2[(Cp'''Co)_2(\mu,\eta^3\text{:}\eta^3\text{-}P_8)]$ (**2a**) can be obtained as a dark green solid in crystalline yields of 40% (Scheme 2). Although well-diffracting single crystals of **2a** could be obtained, a satisfactory refinement of the X-ray data

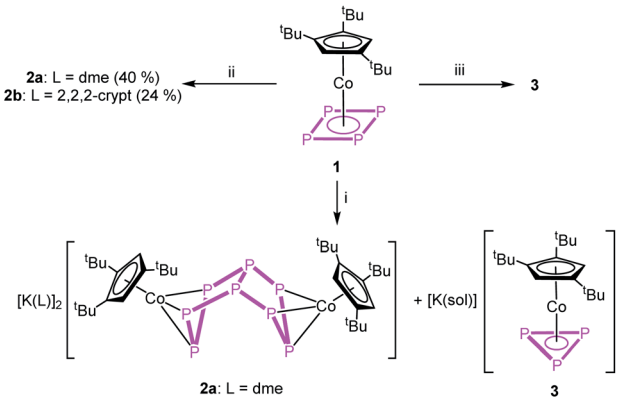

Scheme 2 Reaction of **1** with (i) K, KH or KC_8 in thf at r.t., (ii) $K[CpFe(CO)_2]$ in thf at −80 °C and (iii) with K, KH or KC_8 in thf at r.t. in the presence of 18-c-6 or 2,2,2-cryptand.

was not possible since the potassium counterions and dme molecules are severely disordered over several positions with side occupancies partially below 8% (*cf.* ESI†). The addition of 2,2,2-cryptand to a crude reaction mixture of **2a** and the recrystallization from a dme/acetonitrile mixture at −30 °C yielded single crystals of $[K(2,2,2\text{-cryptand})]_2[(Cp'''Co)_2(\mu,\eta^3\text{:}\eta^3\text{-}P_8)]$ (**2b**) suitable for X-ray diffractions in 24% yield. Both **2a** and **2b** can be isolated as dark green solids that are extremely air- and moisture-sensitive. The structure in the solid state (Fig. 1) shows a dianionic dinuclear complex with a P_8 ligand consisting of a *cis*-bicyclo[3.3.0]octane core that coordinates to two $\{Cp'''Co\}$ fragments. Compound **2** displays the first compound possessing such a ligand. The structural motif is similar to the realgar-like P_8 cages (tricyclo[3.3.0.0]octane) as in $[(L_nM)_4(\mu_4,\eta^1\text{:}\eta^1\text{:}\eta^1\text{:}\eta^1\text{:}\eta^1\text{:}\eta^1\text{:}\eta^1\text{:}\eta^1\text{-}P_8)]$ (L_n-M = nacnacGa,[29] nacnacFe,[30] $NN^{fc}Sc$,[31] Cp^*_2Sm[32]), $[(Cp^{Me}Fe(CO)_2)_2(Cp^{Me}Fe(CO))_2(\mu_4,\eta^1\text{:}\eta^1\text{:}\eta^1\text{:}\eta^1\text{:}\eta^1\text{:}\eta^1\text{-}P_8)]$,[33] $[(Cp^*Ir(CO))_2(\mu_5,\eta^1\text{:}\eta^1\text{:}\eta^1\text{:}\eta^1\text{:}\eta^1\text{:}\eta^1\text{:}\eta^1\text{-}P_8)\{Cr(CO)_5\}_3]$[34] or $[(Cp'''Ni)_2(\mu,\eta^2\text{:}\eta^2\text{-}P_8)]^{2-}$,[5] with the difference that in **2b** one P–P bond is cleaved (P1–P5, Fig. 1). In all mentioned complexes, the P_8 ligands coordinate either in an $\eta^1\text{:}\eta^1$ (Ga, Fe, Sc, Sm, Ir) or η^2 (Ni) fashion to the metal fragments, while in **2b** two allylic P_3 subunits (P1–P2 2.1554(6), P1–P8

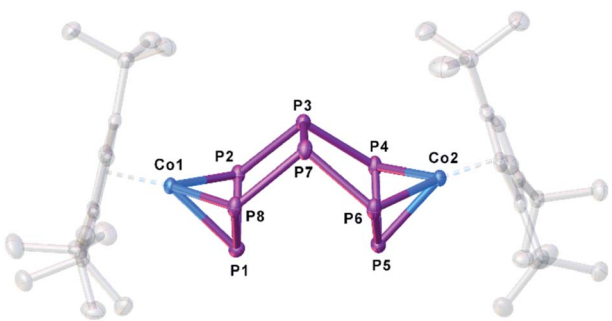

Fig. 1 Structure of the dianion in **2b** in the solid state. Thermal ellipsoids are shown at 50% probability level. Hydrogen atoms, cations and solvent molecules are omitted for clarity.

2.1577(6), P4–P5 2.1519(6), P5–P6 2.1580(6) Å) coordinate to two {Cp‴Co} fragments in an η^3 fashion. These P–P bond lengths are between single[35] and double[36] bond lengths, in line with the calculated Wiberg Bond Indices (WBIs) of 1.11 and 1.12, respectively.

All other P–P distances are in the range of single bonds (2.1947(6)–2.2247(6) Å), which is underlined by WBIs between 0.93 and 0.96. The ^{1}H NMR spectrum of **2a** in thf-d_8 shows three singlets centred at δ = 3.96, 1.31 and 1.22 ppm with an integral ratio of 4 : 36 : 18 indicating two equivalent freely rotating Cp‴ ligands. The $^{31}P\{^1H\}$ NMR spectrum in thf-d_8 shows three multiplets centred at δ = 96.2, 83.1 and −124.2 ppm with an integral ratio of 2 : 4 : 2 of an AA′MM′M″M‴XX′ spin system.

Instead of adding electrons to the system by reduction, nucleophiles can also serve as electron donors. We selected ^{t}BuLi as a strong carbon-based nucleophile with a higher steric demand to avoid side reactions. The reaction with **1** in thf at −80 °C proceeds instantly during the addition of ^{t}BuLi indicated by an immediate colour change from red to brown. After warming to room temperature, the ^{1}H and $^{31}P\{^1H\}$ NMR spectra reveal the selective formation of $[Cp'''Co(\eta^3\text{-}P_4{}^tBu)]^-$ (**4**) (Scheme 3). Pure **4** can be precipitated from the reaction mixture in a yield of 48% after addition of 2,2,2-cryptand.

Regardless of numerous attempts to obtain single crystals of **4** suitable for X-ray diffractions, we were only able to receive poorly diffracting ones (resolution < 1.20 Å). The atom connectivity can be determined unambiguously, a discussion of the bond lengths and angles, however, would not be appropriate. The solid-state structure (*cf.* Fig. S22†) reveals a folded *cyclo*-P_4 ligand with one P atom deviating from the former planar P_4 unit, to which the ^{t}Bu substituent is bonded in an axial position (isomer **4a**). Theoretically, a second isomer with the ^{t}Bu substituent in an equatorial position (**4b**) would be possible, it could, however, not be detected by NMR spectroscopy (*vide infra*; *cf.* Fig. S4†). According to DFT calculations, the energy difference between the axial and equatorial isomers of **4** (*i.e.* **4a** and **4b**) is 11.91 kJ mol^{-1}, with **4a** being favoured. During the optimization of the crystallization conditions, we noticed that **4** is not stable in solution over time (especially in the absence of 2,2,2-cryptand) and is converted to $[(Cp'''Co)_2(\text{-}\mu,\eta^3\text{:}\eta^3\text{-}P_8{}^tBu)]^-$ (**5**) or $[Cp'''Co(\eta^3\text{-}P_3)]^-$ (**3**) and $[Cp'''Co(\eta^3\text{-}P_5{}^tBu_2)]^-$ (**6**) (Scheme 3). This process was monitored by $^{31}P\{^1H\}$ NMR spectroscopy and the products **5** and **6** could be isolated and characterized spectroscopically and by single crystal X-ray diffractions.

For compound **5**, few single crystals suitable for X-ray diffractions could be obtained, while the quality of the crystals of **6** gave only very poor data indicating, however, the atom connectivity in **6** (*cf.* ESI†). The molecular structure of **5** (Fig. 2) shows a binuclear complex with a substituted $P_8{}^tBu$ ligand coordinating to two {Cp‴Co} fragments, each in an η^3 fashion similar to **2**. All P–P distances are comparable to those in **2**. The identity of **3**, **5** and **6** was further proven by simulation of the related $^{31}P\{^1H\}$ NMR spectra. Performing the reaction of **1** with ^{t}BuLi at room temperature, the $^{31}P\{^1H\}$ NMR spectrum of the reaction mixture in thf-d_8 reveals a mixture of all four compounds **3**, **4**, **5** and **6** beside traces of unknown compounds (Fig. 3). The $^{31}P\{^1H\}$ NMR spectra of **4**, **5** and **6** were simulated independent of this spectrum, since **3**, **5** and **6** could not be separated preparatively from each other.

The formation of **5** can be explained by the reaction of **4** with another equivalent of **1**, which is energetically favoured by 52.48 kJ mol^{-1} (Fig. 4) and probably driven by the decrease of the ring strain. An alternative pathway to the release of ring strain would be the dimerisation of two equivalents of **4** followed by a subsequent fragmentation to form **6** (containing an unprecedented, disubstituted *cyclo*-P_5 ligand) and **3** (containing a *cyclo*-P_3 ligand). This reaction is exothermic by 161.09 kJ mol^{-1}. Interestingly, these subsequent reactions can be avoided or at least slowed down when the lithium counter ion is completely separated from the anion in **4** by *i.e.* the addition of 2,2,2-cryptand.

Since the nucleophile ^{t}BuLi seems to be too strong and induces subsequent reactions, we employed $LiCH_2SiMe_3$ as a weaker and sterically less demanding carbon-based nucleophile in the reaction with **1**.

The reaction of **1** with $LiCH_2SiMe_3$ in thf at −80 °C leads to the formation of $[Cp'''Co(\eta^3\text{-}P_3CH_2SiMe_3)]^-$ (**7**) and, after

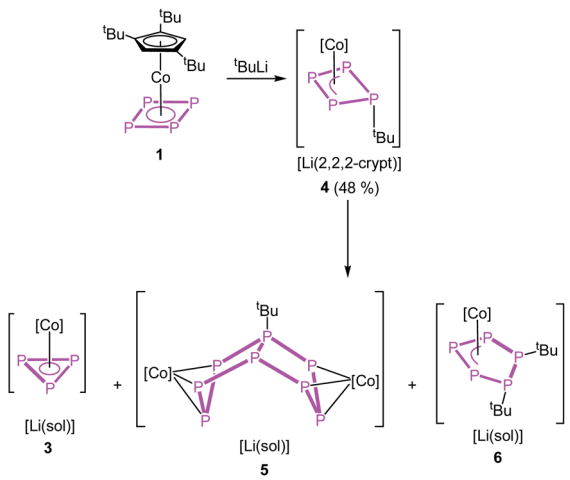

Scheme 3 Reaction of **1** with ^{t}BuLi and subsequent reaction.

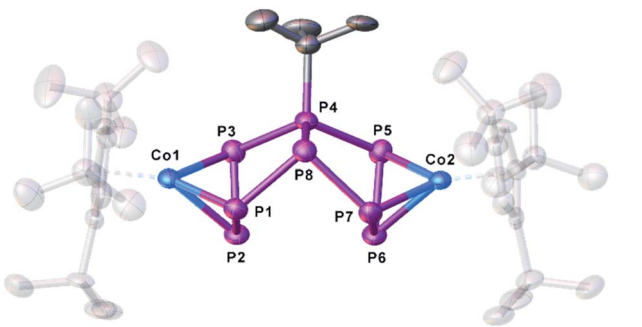

Fig. 2 Molecular structure of the anion of **5** in the solid state. Thermal ellipsoids are shown at 50% probability level. Hydrogen atoms, cations and solvent molecules are omitted for clarity.

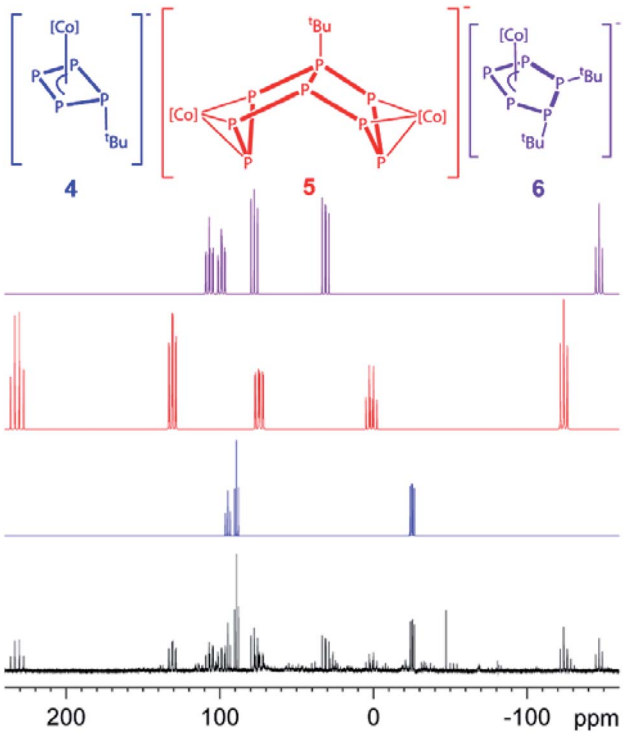

Fig. 3 $^{31}P\{^1H\}$ NMR spectrum of the reaction of **1** with ^{t}BuLi at r.t. in thf-d_8 and the simulated NMR spectra of **4**, **5** and **6** ([Co] = Cp‴Co).

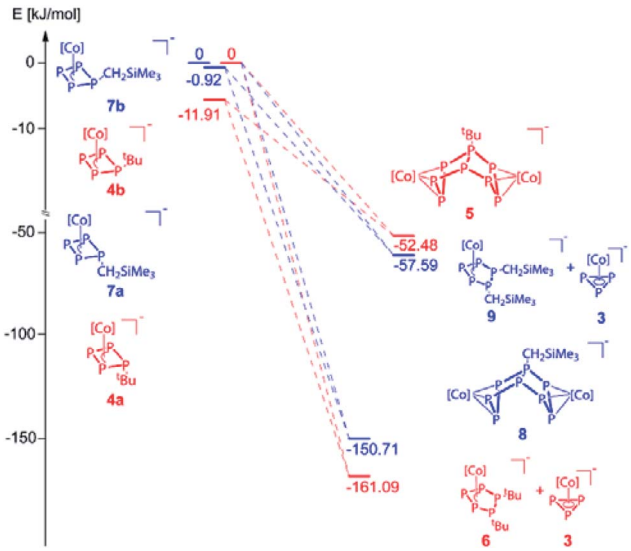

Fig. 4 Energetic diagram of the isomers **4a**,**b** and **7a**,**b** and their subsequent reactions. **4b** and **7b** were each used as reference for the related calculations (0 kJ mol^{-1}, [Co] = Cp‴Co).

warming to room temperature, of $[Li(dme)_3][(Cp'''Co)_2(\mu,\eta^3{:}\eta^3\text{-}P_8CH_2SiMe_3)]$ (**8**), which can be isolated in crystalline yields of 33% after workup (Scheme 4). The formation of **7** and **8** becomes manifest by color changes from red (**1**) to brown (**7**) to green (**8**). The outcome of the reaction is independent of whether 0.5 or 1 equivalents of $LiCH_2SiMe_3$ are used.

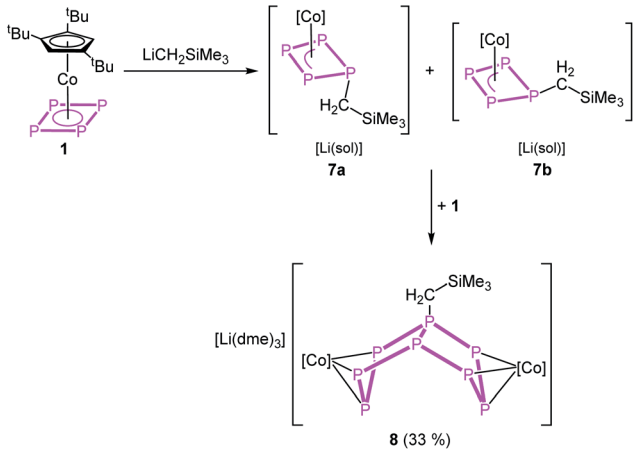

Scheme 4 Reaction of **1** with $LiCH_2SiMe_3$ ([Co] = Cp‴Co).

The reaction can be stopped partially and the formation of **8** be reduced when 12-c-4 or 2,2,2-cryptand is added directly after the addition of $LiCH_2SiMe_3$ at −80 °C. The crude $^{31}P\{^1H\}$ NMR spectra of these reactions reveal two isomers of **7** in a ratio of 1 : 0.25 (2,2,2-crypt) and 1 : 1.33 (12-c-4), respectively, which can be assigned to complexes where the CH_2SiMe_3 substituent is located in an axial position (**7a**) or in an equatorial position (**7b**). The $^{31}P\{^1H\}$ NMR spectra reveal also the formation of **8** and **3** beside minor amounts of unknown side products, while the reaction in the presence of 2,2,2-cryptand seems to be much more selective to giving **3**, **7a**, **7b** and **8** (*cf.* Fig. S10 and S11†). According to DFT calculations, the energy of the isomers **7a** and **7b** differs only by 0.92 kJ mol^{-1}, with **7a** being favoured (Fig. 4). Few crystals of the isomer **7a** were obtained from a concentrated solution of the mixture of isomers in thf layered with *n*-hexane at −30 °C. The molecular structure (Fig. 5, left) shows a folded *cyclo*-P_4 ligand with one P atom bent out of the plane bearing the CH_2SiMe_3 substituent. The P1–P2 (2.2283(16) Å) and P1–P4 (2.2229(19) Å) distances are longer than the P2–P3 (2.1877(17) Å) and P3–P4 (2.1895(16) Å) bonds. All P–P bond lengths are elongated compared to **1**.[14] The $^{31}P\{^1H\}$ NMR spectrum of **7** in thf-d_8 shows three multiplets of an AMXX′ spin system (**7a**) centred at δ = 52.6, 46.0 and 18.8 ppm with an integral ratio of 1 : 1 : 2 and three multiplets of an AMM′X spin system (**7b**) centred at δ = 39.5, 3.94 and −78.0 ppm with an integral ratio of

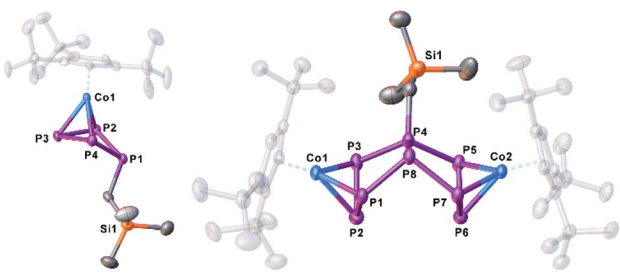

Fig. 5 Molecular structure of the anions **7a** and **8** in the solid state. Thermal ellipsoids are shown at 50% probability level. Hydrogen atoms, cations and solvent molecules are omitted for clarity.

1 : 2 : 1. The J_{PP} coupling constants obtained from the simulation (*cf.* ESI†) correlate nicely with the bond distances obtained from the X-ray structure determination.

When the reaction is conducted without the use of 12-c-4 or 2,2,2-cryptand, a colour change from initial red to brown (**7**) to dark green (**8**) is observed. Crystals of **8** suitable for single crystal X-ray diffraction were obtained from a concentrated solution in a mixture of *n*-hexane and dme stored at −30 °C. The structure of **8** (Fig. 5, right) shows a dinuclear anionic complex with a substituted P_8 ligand. The P_8 structural motif is similar to that observed in the reduced complex **2** and analogous to that found in **5**. The P_8 ligand consists of two condensed five-membered rings (bicyclo[3.3.0]octane) coordinating to the {Cp‴Co} fragments *via* the allylic P_3 subunits (P1–P2–P3 and P5–P6–P7). The bond distances (P1–P2 2.1643(11), P2–P3 2.1574(11), P5–P6 2.1494(11), P6–P7 2.1575(11) Å) are in the range between single and double bonds, indicated by the WBIs between 1.09 and 1.11. All other P–P distances are in the range of single bonds. The $^{31}P\{^1H\}$ NMR spectrum of **8** in thf-d_8 shows five multiplets centred at δ = 187.9, 102.8, 74.4, 40.6 and −118.8 ppm with an integral ratio of 1 : 2 : 2 : 1 : 2 indicating an $AM_2N_2OX_2$ spin system. The simulation of the spectrum at 193 K was conducted to determine the coupling constants and chemical shifts (*cf.* Fig. S13†). The formation of **8** can be explained by the reaction of **7** with another equivalent of **1**, energetically favoured by −150.71 kJ mol^{-1}. Alternatively, as also might be true for the formation of **5**, a formal intermolecular nucleophilic attack of **7** at another molecule **7** under release of $LiCH_2SiMe_3$ to **8** (S_N2 type), which is supported by the VT $^{31}P\{^1H\}$ NMR of the reaction between **1** and $LiCH_2SiMe_3$ (*cf.* Fig. S14–S16†). At 193 K, the reaction is already complete (absence of signals of **1**). The $^{31}P\{^1H\}$ NMR spectrum shows six broad multiplets that can be assigned to **7a**,**b**. Upon warming, these signals broaden and only two broad triplets remain (at 233 and 253 K). The formation of **8** is detected for the first time at 253 K. At room temperature, **3**, **7a**,**b**, **8** and a second set of signals quite similar to those of **8** are observed. The latter might represent an isomer of **8** (starting either from **7a** or **7b**). After 24 hours at room temperature, the signals of **7a**,**b** disappeared completely. Interestingly, whereas the formation of **6** as an additional product of the reaction between **1** and ^{t}BuLi was found, the corresponding product $[Cp'''Co(\eta^3\text{-}P_5(CH_2SiMe_3)_2)]^-$ (**9**) for the reaction of **1** with $LiCH_2SiMe_3$ could never be detected by NMR, since the dimerisation and subsequent fragmentation of **7** to **9** and **3** would be energetically less favoured (−57.59 kJ mol^{-1}; Fig. 4). Beside the relative thermodynamic stability of the intermediates **4** and **7**, the kinetic effects of the transformation processes play an important role, which is indicated by the outcome of these reactions, as well as their conversion rates.

The reaction of the oxygen-based nucleophile NaOH with **1** at room temperature yields $[Na(dme)_3][Cp'''Co(\eta^3\text{-}P_4(O)H)]$ (**10**) in crystalline yields of 55% after workup (eqn (1)). In the first step, OH^- binds to one phosphorus atom of the *cyclo*-P_4 ligand in **1**, followed by a proposed tautomeric rearrangement with the formation of a P=O double and P–H single bond.

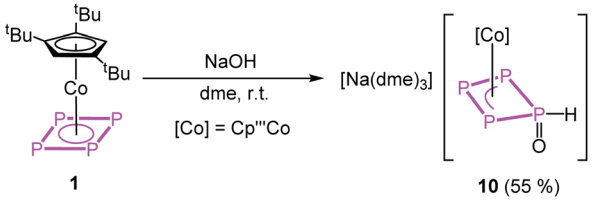

1 **10** (55 %) (1)

The structure of **10** (Fig. 6) reveals a folded *cyclo*-P_4 ligand in which one P atom is bent out of the plane (P1). The hydrogen atom bonded to phosphorus (H1) was found on the electron density map and was freely refined. The P–P distances are in the range of single or slightly shortened single bonds (P1–P2 2.1659(7), P1–P4 2.1676(7), P2–P3 2.1984(8), P3–P4 2.1938(8) Å; WBIs 0.94–1.07). The P1–O1 bond (1.5200(15) Å) is in the range between a single and a double bond (WBI of 1.08).

The $^{31}P\{^1H\}$ NMR spectrum of **10** in thf-d_8 shows three multiplets centred at δ = 74.5, 29.0 and −21.8 ppm with an integral ratio of 2 : 1 : 1 indicating an A_2MX spin system. In the ^{31}P NMR spectrum, a coupling between H1 and all P atoms can be observed. In the ^1H NMR spectrum, a doublet of triplet of doublets at 7.78 ppm with the coupling constants of $^1J_{PH}$ = 356.8, $^2J_{PH}$ = 20.6 and $^3J_{PH}$ = 5.1 Hz could be detected among the characteristic signals for the Cp‴ ligand. A similar reaction was reported by Peruzzini and co-workers for the reaction of $[Ir(dppm)(Ph_2PCH_2PPh_2PPPP)]^+$ with water under basic conditions.[37]

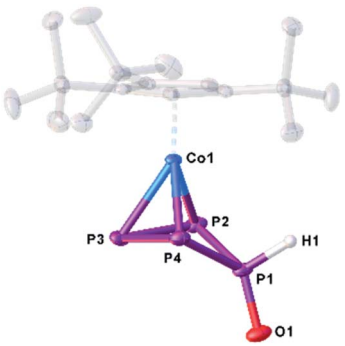

Fig. 6 Molecular structure of the anion in **10** in the solid state. Thermal ellipsoids are shown at 50% probability level. Hydrogen atoms, cations and solvent molecules are omitted for clarity.

Conclusions

In summary, we were able to show that the irreversible dimerisation reaction of **1** can be overcome by carrying out the reactions at room temperature or lower. That way, in reactions with main group nucleophiles and upon reduction, **1** displays a unique tendency to release the ring strain of the *cyclo*-P_4 ligand. Here, unprecedented aggregation and rearrangement processes occur. The reduction of **1** with $K[CpFe(CO)_2]$ yields selectively the dinuclear dianionic complex $[(Cp'''Co)_2(\mu,\eta^3\text{:}\eta^3\text{-}P_8)]^{2-}$ (**2**), comprising an unprecedented open realgar-like P_8 cage that reveals a double η^3-coordinated P_8 ligand for the first

time. Compound **1** was functionalised with the main group nucleophiles ^{t}BuLi and $LiCH_2SiMe_3$, respectively, and $[Cp'''Co(\eta^3\text{-}P_4R)]^-$ (R = ^{t}Bu (**4**), CH_2SiMe_3 (**7**)) could be isolated as the first reaction products. Both compounds are metastable and show further rearrangement processes such as dimerisation and/or fragmentation. In comparison to other nucleophile-substituted polyphosphorus complexes starting from a four-membered ring in **1**, here the first-formed product is highly reactive. Thus, compounds **4** and **7** can act as nucleophiles and react with another equivalent of **1** to the dinuclear complexes $[(Cp'''Co)_2(\mu,\eta^3\text{:}\eta^3\text{-}P_8R)]^-$ (R = ^{t}Bu (**5**), CH_2SiMe_3 (**8**)) comprising novel organo-substituted open realgar-like P_8R ligands. For **4**, an additional reaction pathway was observed. The formal dimerisation of **4** followed by an unprecedented fragmentation gives $[Cp'''Co(\eta^3\text{-}P_5{}^tBu_2)]^-$ (**6**) with a new diorgano-substituted *cyclo*-P_5 ligand and $[Cp'''Co(\eta^3\text{-}P_3)]^-$ (**3**).

Conflicts of interest

There are no conflicts to declare.

Acknowledgements

This work was supported by the Deutsche Forschungsgemeinschaft within the project Sche 384/38-1 and Sche 384/33-2. M. P. is grateful to the Fonds der Chemischen Industrie for a PhD fellowship.

Notes and references

1 Examples for complexes with a C_4H_4 ligand: (*a*) P. D. Harvey, W. P. Schaefer, H. B. Gray, D. F. R. Gilson and I. S. Butler, *Inorg. Chem.*, 1988, **27**, 57; (*b*) L. M. Cirjak, J.-S. Huang, Z.-H. Zhu and L. F. Dahl, *J. Am. Chem. Soc.*, 1980, **102**, 6623; (*c*) P. E. Riley and R. E. Davis, *J. Organomet. Chem.*, 1977, **137**, 91; (*d*) R. E. Davis and P. E. Riley, *Inorg. Chem.*, 1980, **19**, 674; (*e*) P. E. Riley and R. E. Davis, *J. Organomet. Chem.*, 1976, **113**, 157. For C_3H_3 no examples were found in the CSD data bank. For more stable substituted derivatives with C_3R_3 (R = alkyl, aryl, *e.g.* R. M. Tuggle and D. L. Weaver, *Inorg. Chem.* 1971, **10**, 1504) and C_4R_4 ligands (R = alkyl, aryl, *e.g.* A. R. Kudinov, E. V. Mutseneck and D. A. Luginov, *Coord*. Chem. Rev. 2004, **248**, 571) are known and studied.

2 (*a*) R. S. P. Turbervill, A. R. Jupp, P. S. B. McCullough, D. Ergöçmen and J. M. Goicoechea, *Organometallics*, 2013, **32**, 2234; (*b*) F. Nief and L. Ricard, *Organometallics*, 2001, **20**, 3884; (*c*) S. Du, Z. Chai, J. Hu, W.-X. Zhang and Z. Xi, *Chin. J. Org. Chem.*, 2019, **39**, 2338; (*d*) S. Du, J. Yin, Y. Chi, L. Xu and W.-X. Zhang, *Angew. Chem., Int. Ed.*, 2017, **56**, 15886; (*e*) S. Du, J. Yang, J. Hu, Z. Chai, G. Luo, Y. Luo, W.-X. Zhang and Z. Xi, *J. Am. Chem. Soc.*, 2019, **141**, 6843.

3 C. Elschenbroich, M. Nowotny, B. Metz, W. Massa, J. Graulich, K. Biehler and W. Sauer, *Angew. Chem., Int. Ed. Engl.*, 1991, **30**, 547.

4 O. J. Scherer, J. Braun and G. Wolmershäuser, *Chem. Ber.*, 1990, **123**, 471.

5 E. Mädl, G. Balázs, E. V. Peresypkina and M. Scheer, *Angew. Chem., Int. Ed.*, 2016, **55**, 7702.

6 O. J. Scherer and T. Brück, *Angew. Chem., Int. Ed. Engl.*, 1987, **26**, 59.

7 O. J. Scherer, T. Brück and G. Wolmershäuser, *Chem. Ber.*, 1988, **121**, 935.

8 (*a*) L. Y. Goh, R. C. S. Wong, C. K. Chu and T. W. Hambley, *J. Chem. Soc., Dalton Trans.*, 1990, **6**, 977; (*b*) O. J. Scherer, J. Schwalb, G. Wolmershäuser, W. Kaim and R. Gross, *Angew. Chem., Int. Ed. Engl.*, 1986, **25**, 363.

9 S. Heinl, G. Balázs, M. Bodensteiner and M. Scheer, *Dalton Trans.*, 2016, **45**, 1962.

10 O. J. Scherer, H. Swarowsky, G. Wolmershäuser, W. Kaim and S. Kohlmann, *Angew. Chem., Int. Ed. Engl.*, 1987, **26**, 1153.

11 O. J. Scherer, J. Schwalb, H. Swarowsky, G. Wolmershäuser, W. Kaim and R. Gross, *Chem. Ber.*, 1988, **121**, 443.

12 O. J. Scherer, J. Vondung and G. Wolmershäuser, *Angew. Chem., Int. Ed. Engl.*, 1989, **28**, 1355.

13 (*a*) M. Fleischmann, C. Heindl, M. Seidl, G. Balázs, A. V. Virovets, E. V. Peresypkina, M. Tsunoda, F. P. Gabbaï and M. Scheer, *Angew. Chem., Int. Ed.*, 2012, **51**, 9918; (*b*) M. Fleischmann, F. Dielmann, G. Balázs and M. Scheer, *Chem.–Eur. J.*, 2016, **22**, 15248; (*c*) O. J. Scherer, H. Sitzmann and G. Wolmershäuser, *Angew. Chem., Int. Ed. Engl.*, 1985, **24**, 351.

14 F. Dielmann, A. Timoshkin, M. Piesch, G. Balázs and M. Scheer, *Angew. Chem., Int. Ed.*, 2017, **56**, 1671.

15 (*a*) C. Schoo, S. Bestgen, M. Schmidt, S. N. Konchenko, M. Scheer and P. W. Roesky, *Chem. Commun.*, 2018, **54**, 4770; (*b*) L. Qiao, C. Zhang, X.-W. Zhang, Z.-C. Wang, H. Yin and Z.-M. Sun, *Chin. J. Chem.*, 2020, **38**, 295.

16 (*a*) O. J. Scherer, R. Winter and G. Wolmershäuser, *Z. Anorg. Allg. Chem.*, 1993, **619**, 827; (*b*) M. Herberhold, G. Frohmader and W. Milius, *J. Organomet. Chem.*, 1996, **522**, 185.

17 C. Schwarzmaier, A. Noor, G. Glatz, M. Zabel, A. Y. Timoshkin, B. M. Cossairt, C. C. Cummins, R. Kempe and M. Scheer, *Angew. Chem., Int. Ed.*, 2011, **50**, 7283.

18 A. Cavaillé, N. Saffon-Merceron, N. Nebra, M. Fustier-Boutignon and N. Mézailles, *Angew. Chem., Int. Ed.*, 2018, **57**, 1874.

19 K. A. Mandla, C. E. Moore, A. L. Rheingold and J. S. Figueroa, *Angew. Chem., Int. Ed.*, 2018, **57**, 6853.

20 U. Chakraborty, J. Leitl, B. Mühldorf, M. Bodensteiner, S. Pelties and R. Wolf, *Dalton Trans.*, 2018, **47**, 3693.

21 C. M. Hoidn, T. M. Maier, K. Trabitsch, J. J. Weigand and R. Wolf, *Angew. Chem., Int. Ed.*, 2019, **58**, 18931.

22 F. Dielmann, E. V. Peresypkina, B. Krämer, F. Hastreiter, B. P. Johnson, M. Zabel, C. Heindl and M. Scheer, *Angew. Chem., Int. Ed.*, 2016, **55**, 14833.

23 (*a*) M. Piesch, M. Seidl, M. Stubenhofer and M. Scheer, *Chem.–Eur. J.*, 2019, **25**, 6311; (*b*) G. Capozzi, L. Chiti, M. Di Vaira, M. Peruzzini and P. Stoppioni, *J. Chem. Soc., Chem. Commun.*, 1986, 1799; (*c*) P. Barbaro, A. Ienco, C. Mealli, M. Peruzzini, O. Scherer, G. Schmitt, F. Vizza and G. Wolmershäuser, *Chem.–Eur. J.*, 2003, **9**, 5195.

24 E. Mädl, M. V. Butovskii, G. Balázs, E. V. Peresypkina, A. V. Virovets, M. Seidl and M. Scheer, *Angew. Chem., Int. Ed.*, 2014, **53**, 7643.
25 J. R. Corfield, M. J. P. Harger, J. R. Shutt and S. Trippett, *J. Chem. Soc. C*, 1970, 1855.
26 E.-M. Rummel, G. Balázs, V. Heinl and M. Scheer, *Angew. Chem., Int. Ed.*, 2017, **56**, 9592.
27 $[Cp'''Co(\eta^3\text{-}P_3)]-$ was obtained by the reaction of **1** with ^{Me}NHC (1,3,4,5-tetramethyl-imidazol-2-ylidene): M. Piesch, S. Reichl, M. Seidl, G. Balázs and M. Scheer, *Angew. Chem., Int. Ed.*, 2019, **58**, 16563.
28 N. G. Connelly and W. E. Geiger, *Chem. Rev.*, 1996, **96**, 877.
29 F. Hennersdorf, J. Frötschel and J. J. Weigand, *J. Am. Chem. Soc.*, 2017, **139**, 14592.
30 F. Spitzer, C. Graßl, G. Balázs, E. M. Zolnhofer, K. Meyer and M. Scheer, *Angew. Chem., Int. Ed.*, 2016, **55**, 4340.
31 W. Huang and P. L. Diaconescu, *Chem. Commun.*, 2012, **48**, 2216.
32 S. N. Konchenko, N. A. Pushkarevsky, M. T. Gamer, R. Köppe, H. Schnöckel and P. W. Roesky, *J. Am. Chem. Soc.*, 2009, **131**, 5740.
33 M. E. Barr, B. R. Adams, R. R. Weller and L. F. Dahl, *J. Am. Chem. Soc.*, 1991, **113**, 3052.
34 M. Scheer, U. Becker and E. Matern, *Chem. Ber.*, 1996, **129**, 721.
35 P. Pyykkö and M. Atsumi, *Chem.–Eur. J.*, 2009, **15**, 186.
36 P. Pyykkö and M. Atsumi, *Chem.–Eur. J.*, 2009, **15**, 12770.
37 V. Mirabello, M. Corpali, L. Gonsalvi, G. Manca, A. Ienco and M. Peruzzini, *Chem.–Asian J.*, 2013, **8**, 3177.